21. International winter meeting on nuclear physics
Bormio, Italy 24-29 Jan 1983
CEA-CONF--6651

FR8302727

PROJECTILE FRAGMENTATION AND LIGHT PARTICLE EMISSION FROM 70 MeV/NUCLEON α PARTICLES ON ^{197}Au

Y. Blumenfeld*, Y. Cassagnou, M. Conjeaud, R. Dayras, S. Harar, R. Legrain, M.S. Nguyen, E.C. Pollacco, C. Volant and J.P. Wieleczko

DPh-N/BE, CEN Saclay, 91191 Gif-sur-Yvette cedex, France

Abstract

Light particles (p,d,t,^{3}He) energy spectra from 70 MeV/nucleon α on ^{197}Au have been measured at angles ranging from 10° to 30° in the laboratory. The results have been analysed in terms of fragmentation and moving thermal source models. It is shown that α induced data display similar features as heavy ions data.

**IPN Orsay, BP n°1, 91406 Orsay, France*

Introduction

Projectile fragmentation [1-4] and light particle emission [4-7] from heavy ions collisions in the energy range from about 20 MeV/nucleon to 100 MeV/nucleon are presently of particular interest. In order to investigate the suitability of α particles as projectiles for studying these reaction mechanisms in this energy range, we have detected the light ejectiles from the $\alpha + {}^{197}Au$ reaction at 280 MeV. Preliminary results are presented in this report.

Experimental procedure

A 280 MeV α particle beam ($\sim 2 \times 10^{10}$ α/s) delivered by the synchrotron SATURNE was used to bombard a 1.5 mg/cm^2 gold target. Light particles were detected in a telescope consisting of a ΔE silicon detector (2000 μ thick) and a E NaI(Tl) crystal (4" thick). Particle identification from ΔE-E measurements was good as can be seen from fig.1. Energy calibration of the NaI detector was established using elastically scattered and energy degraded particles. Energy spectra were measured at angles ranging from 10° to 30° in the laboratory.

Results and discussion

Energy spectra for protons deuterons tritons and ^{3}He are presented in fig. 2. A general feature of these spectra is the presence of a high energy tail decreasing exponentially with energy. However for the most forward angles a broad bump centered at an energy corresponding to the beam velocity can be clearly distinguished.

In fig.3 contours of Lorentz invariant iso cross sections are plotted in the rapidity ($y = \frac{1}{2} \log \frac{E + P_{/\!/}}{E - P_{/\!/}}$) transverse velocity plane for protons and tritons. From these rapidity plots, it can be seen that two sources contribute to the cross section. One source has a rapidity close to the projectile rapidity while the other source seems to be located at a rapidity intermediate between target and projectile.

It can also be noted that for tritons, the transverse momentum width of the beam velocity component is larger than the longitudinal momentum width. All these characteristics are quite similar to those observed for heavy ions collisions so we have used the same methods of analysis as for heavy ions. In particular we have fitted the high energy side of the protons energy spectrum at 10° with a gaussian in momentum space [8] :

$$\frac{d^3\sigma}{d^3p} \propto \exp\left(\frac{-(P-P_0)^2}{2\sigma^2}\right)$$

where p_0 is the momentum corresponding to the center of the distribution and

$$\sigma^2 = \frac{F(A-F)}{A-1} \sigma_0^2$$

A and F are the projectile and fragment mass numbers respectively and σ_0 is a reduced momentum width characterizing the intrinsic motion of the nucleons in the nucleus. It is possible to reproduce the proton data with a value of $\sigma_0 \simeq$ 65-70 MeV/c which is not very different from the width that can be deduced from higher energy measurement [9,10] ($\langle P^2\rangle^{1/2} = \sqrt{3}\,\sigma_0 = 130$ MeV/c $\rightarrow \sigma_0 = 75$ MeV/c).

We then performed a two component fit to all the protons spectra. One component was described by the fragmentation model with $\sigma_0 = 65$ MeV/c and the second component was described in terms of a maxwellian distribution in a frame that moves with a velocity intermediate between target and projectile : [6] (moving source model) :

$$\frac{d^2\sigma}{dEd\Omega} = N_0(E-ZE_c)^{1/2} \exp\left(-(E-ZE_c + E_1 - 2E_1^{1/2}(E-ZE_c)^{1/2} \cos\theta)/T\right)$$

Here ZE_c is the kinetic energy gained by the light particle of charge Z in the Coulomb field of the target, $E_1 = mv^2/2$ is the kinetic energy of a particle at rest in the moving frame, T is the temperature of the moving source, θ is the detection angle and N_0 an overall normalization constant. The results of such a two component fit for protons are shown by the solid lines in fig.2 while the dashed and dotted-dashed curves represent the moving source and fragmentation components at 10° respectively. The temperature of the source extracted from the proton spectra is 11.3 MeV.

Increased transverse momentum widths have already been observed for heavy ions fragmentation around 100 MeV/nucleon [2]. This effect has been attributed to the orbital deflection of the projectile prior to break-up. The orbital deflection gives an additionnal dispersion of the transverse momentum [2,8] :

$$\sigma_\perp^2\ (F) = \frac{F(A-F)}{A-1}\sigma_0^2 + \frac{F(F-1)}{A(A-1)}\sigma_2^2$$

where $\sigma_2^2 = \frac{1}{2}\langle P_{A\perp}{}^2\rangle$ is the variance of the transverse momentum of the projectile at the time of fragmentation. σ_2 can be derived [2] from the calculation of the classical deflection function in the Coulomb and nuclear potentials, assuming a Wood-Saxon form-factor for the nuclear part ($r_0 = 1.2$ fm, $a = 0.6$ fm, $V \simeq 60$ MeV) Another input to the calculation is the ratio of the cross sections σ (fragmentation) / σ tot $\simeq 0.6$ which defines the range of impact parameters b over which the deflection function operates. Then $\sigma_2^2 = \frac{1}{2} P_A{}^2 \int N(b) \sin^2\theta(b)db$ where $N(b) = Z/(R^2-b^2)$ is the weighting factor for impact parameter. This orbital dispersion gives the general trend of the data observed with $\simeq$ 100 MeV/n ^{16}O [2].

We can rewrite the differential cross section in momentum space as :

$$\frac{d^3\sigma}{d^3p} \propto \exp\left(\frac{-(P_{/\!/}-\langle P_{/\!/}\rangle)^2}{2\sigma_{/\!/}^2} - \frac{p^2}{2\sigma_\perp^2}\right)$$

All the deuteron, tritons and ^{3}He spectra were fitted with a two sources model. One component was the moving thermal source the other component was a source with beam velocity and is described by the fragmentation model with

$$\sigma_\perp^2 = \frac{F(A-F)}{A-1}\sigma_o^2 + \frac{F(F-1)}{A(A-1)}\sigma_2^2$$

$$\sigma_{/\!/}^2 = \frac{F(A-F)}{A-1} \quad \text{and} \quad \sigma_o = 65 \text{ MeV/c}$$

The solid lines on fig. 2 represents the results of the fits and the dashed and dotted-dashed lines are the moving source and fragmentation components respectively at 10°.

In fig. 4 the transverse momentum widths extracted from the fits are plotted as a function of the fragment mass number and compared to the predictions of the orbital dispersion model with potentials 40 MeV and 50 MeV deep. In this case the orbital dispersion model also reproduces the general trend of the data.

The temperatures of the moving source for d, t, and ^{3}He extracted temperatures from the fit are 14.1, 16.4 and 14.3 respectively. The temperature obtained for protons is plotted in fig. 5 (taken from ref.[6]) with other temperatures obtained at different incident α energies [11,12].

These temperatures show the same smooth increase with incident energy above the Coulomb barrier as the heavy ion data. It can also be noted that with incident α particles the extracted temperatures from d ant t spectra are higher than the temperature deduced from the proton spectra.

Conclusion

70 MeV/nucleon α particles induced reaction display features very similar to those observed in heavy ions reactions, for projectile fragmentation as well as for light particle emission. This shows that α induced reactions could be a useful tool to study these reaction mechanisms.

REFERENCES

[1] Ch. Egelhaaf et al., Phys. Rev. Lett. 46 (1981) 813.

[2] K. Van Bibber et al. Phys. Rev. Lett. 43 (1979) 840.

[3] J. Mougey et al., Phys. Lett. 105B (1981) 25.

[4] J.B. Natowitz et al., Phys. Rev. Lett. 47 (1981) 1114.

[5] R.L. Auble et al., Phys. Rev. C25 (1982) 2504.

[6] T.C. Awes et al., Phys. Rev. C25 (1982) 2361.

[7] G.D. Westfall et al., Phys. Lett. 116B (1982) 118.

[8] A.S. Goldhaber, Phys. Lett. 53B (1974) 306.

[9] L.M. Anderson, Report LBL 6769.

[10] T. Fujita et al., Nucl. Phys. A343 (1980) 493.

[11] R. Głasow et al., Phys. Lett. 120B (1983) 7.

[12] K.R. Cordell et al. Nucl. Phys. A362 (1981) 43.

FIGURE CAPTIONS

Fig. 1. ΔE–E dot plots for 280 MeV α on ^{197}Au at 30° in the laboratory. Two different ΔE gains are presented.

Fig. 2 p, d, t, ^{3}He energy spectra from 280 MeV α on ^{197}Au. The solid lines represent the results of the fits described in the text. Dashed and dotted dashed lines are for the moving thermal source and fragmentation components respectively.

Fig. 3 Constant contours of Lorentz invariant cross sections in arbitrary units as a function of fragment transverse momentum and rapidity for protons and tritons.

Fig. 4 Transverse momentum widths as a function of fragment mass number.

Fig. 5 Moving source temperatures as a function of the incident energy above the Coulomb barrier per nucleon (tableau from ref. 6).

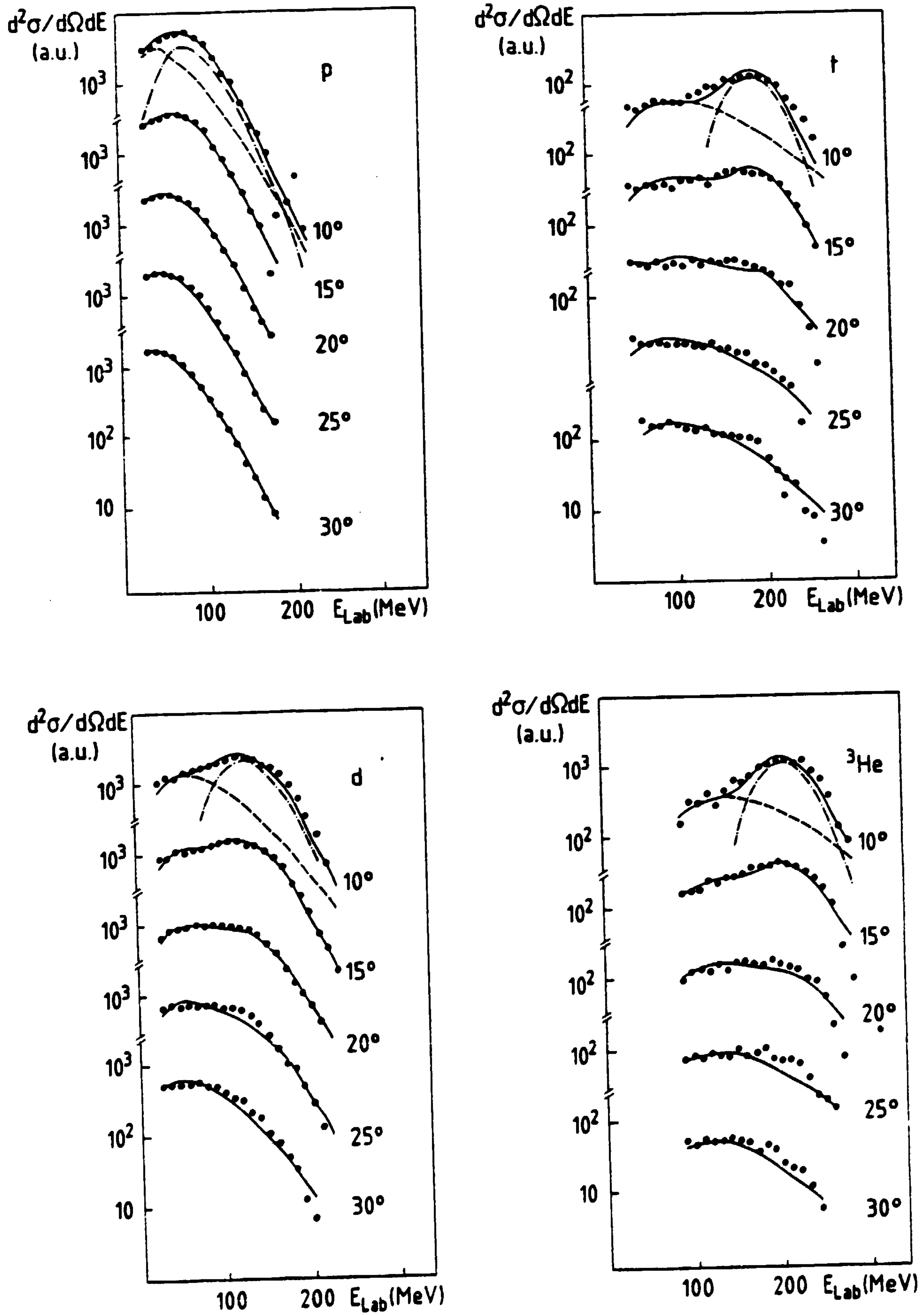

Fig. 1

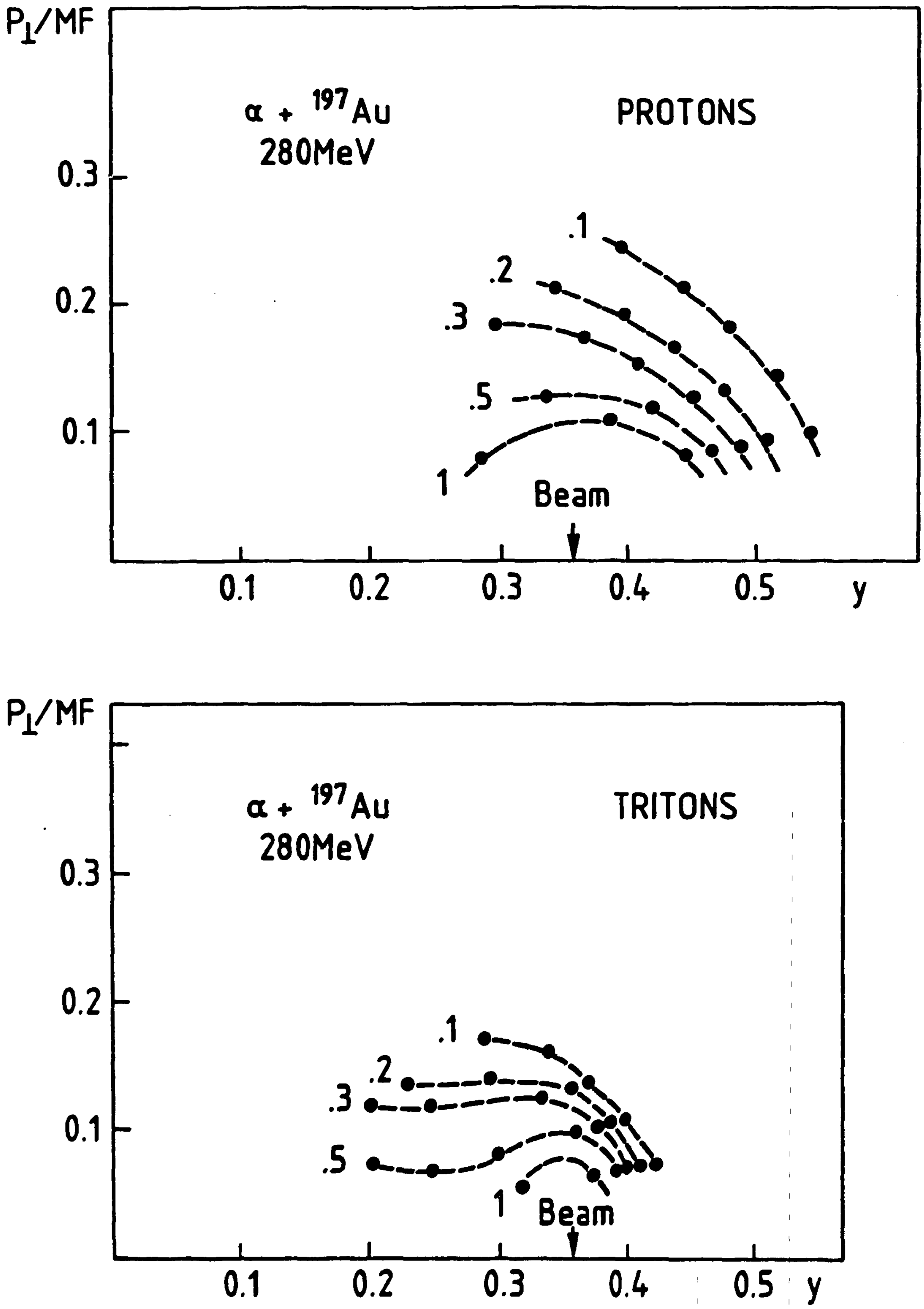
P⊥/MF
α + 197Au
280MeV
PROTONS
0.3
0.2
0.1
.1
.2
.3
.5
1
Beam
0.1
0.2
0.3
0.4
0.5
y
P⊥/MF
α + 197Au
280MeV
TRITONS
0.3
0.2
0.1
.1
.2
.3
.5
1
Beam
0.1
0.2
0.3
0.4
0.5
y

Fig. 2

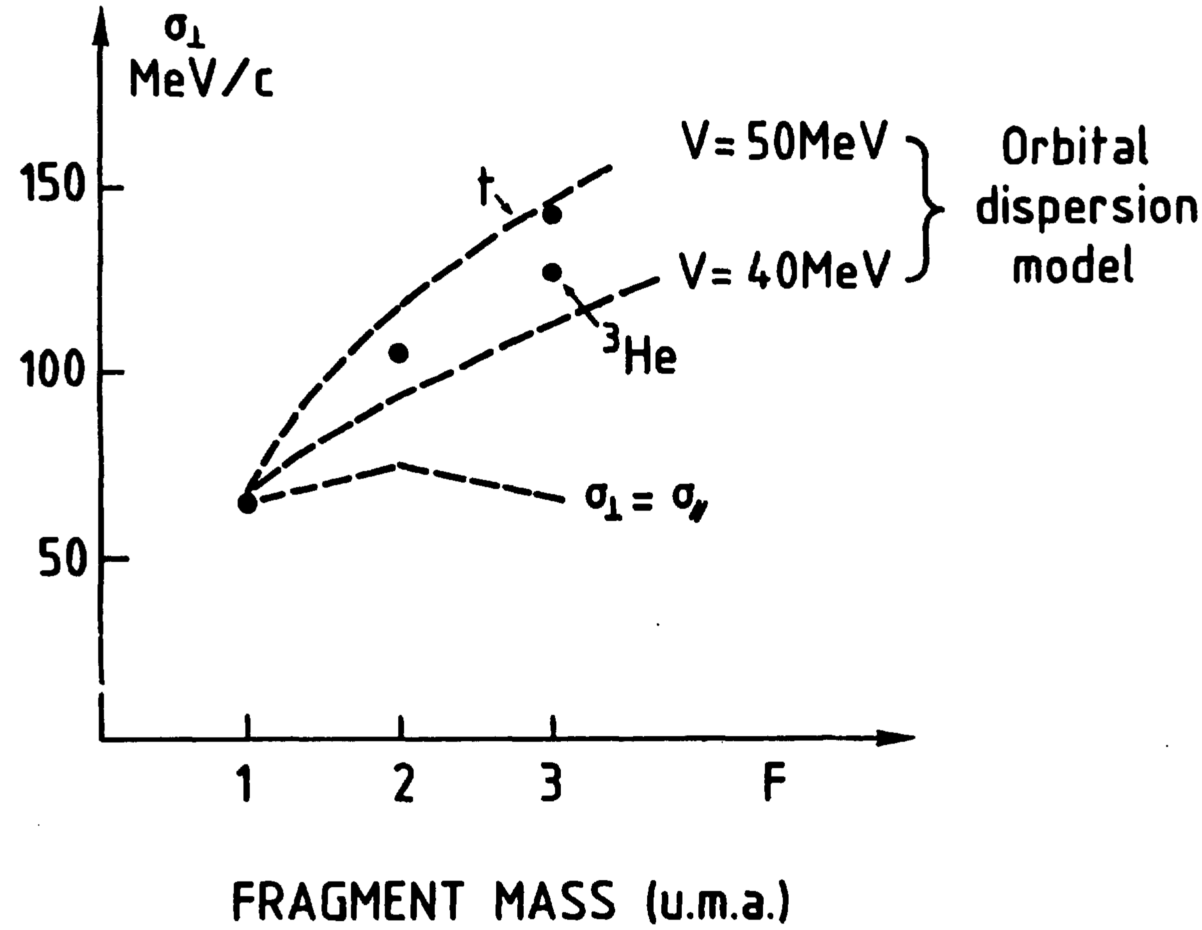
σ⊥
MeV/c
150
100
50
t
3He
V= 50MeV
V= 40MeV
Orbital
dispersion
model
σ⊥ = σ∥
1
2
3
F
FRAGMENT MASS (u.m.a.)

Fig. 3

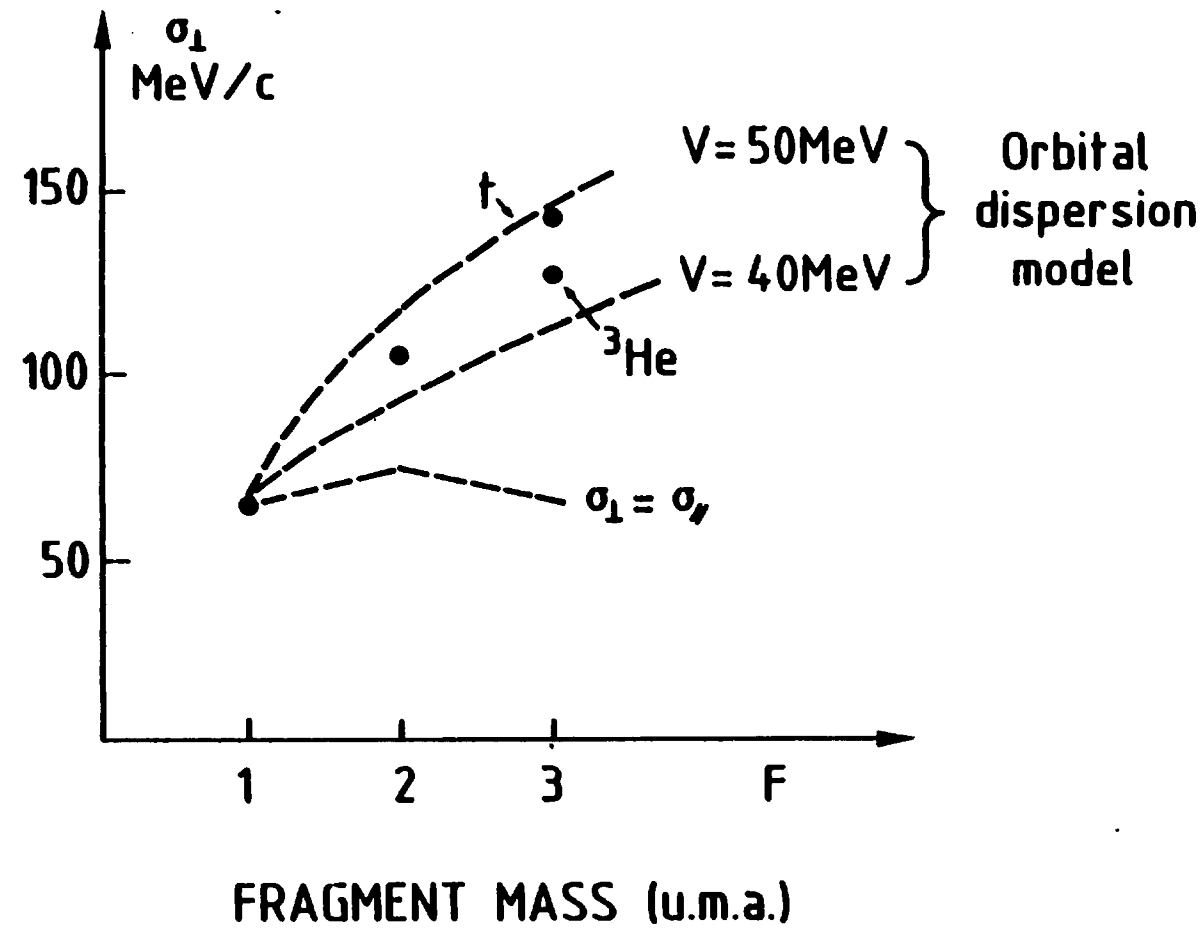

σ⊥
MeV/c
150
100
50
1
2
3
F
t
³He
V= 50MeV
V= 40MeV
Orbital dispersion model
σ⊥ = σ∥
FRAGMENT MASS (u.m.a.)

Fig. 4

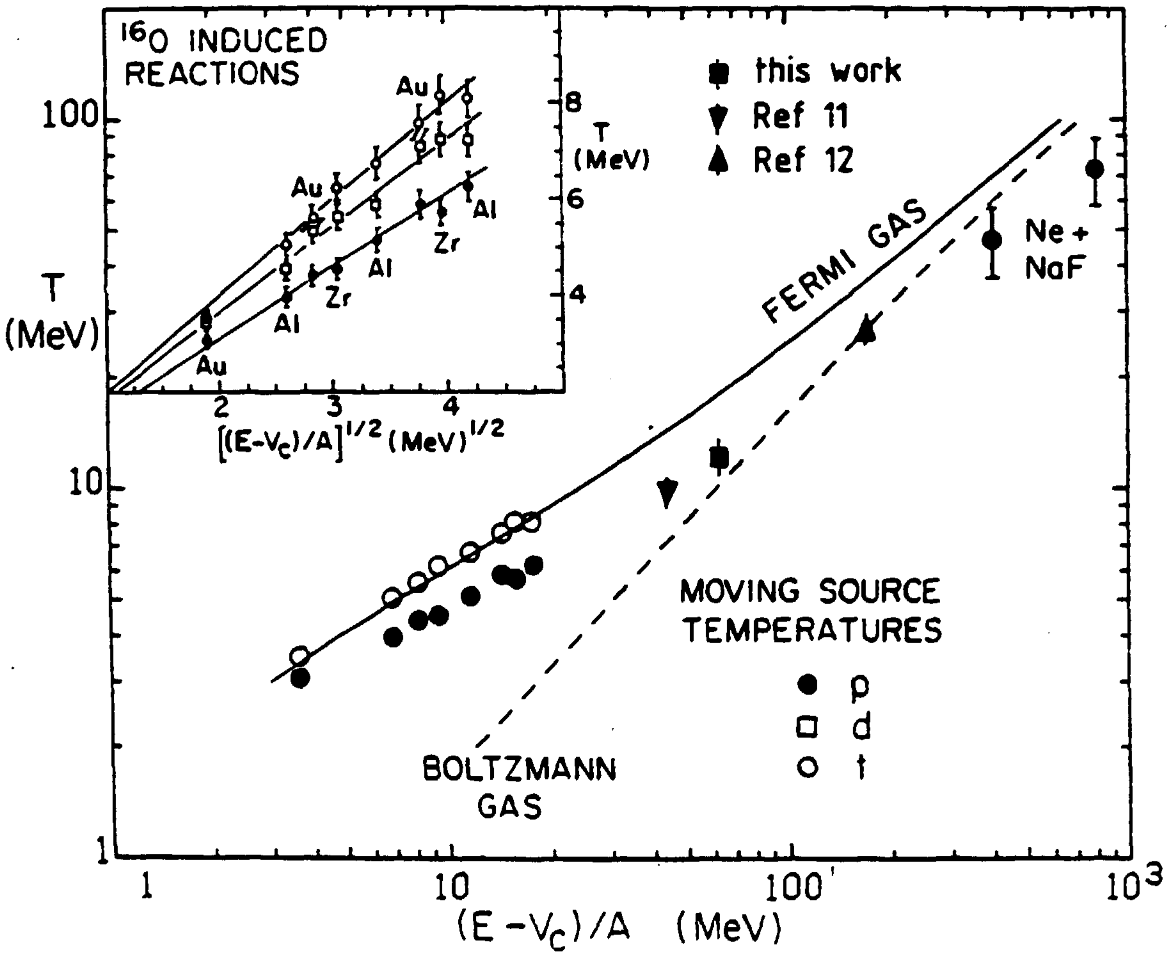

^{16}O INDUCED REACTIONS
this work
Ref 11
Ref 12
T (MeV)
FERMI GAS
Ne + NaF
MOVING SOURCE TEMPERATURES
p
d
t
BOLTZMANN GAS
$[(E-V_c)/A]^{1/2}$ (MeV)$^{1/2}$
$(E-V_c)/A$ (MeV)
Au
Al
Zr